CHARACTERIZATION OF CRYSTALLINE CELLULOSE EXTRACTED FROM DISTILLED WASTE OF *CYMBOPOGON WINTERIANUS*

DISHA MISHRA, PUJA KHARE, M. R. DAS,[*] SHILPA MOHANTY,[**]
D. U. BAWAN KULE[**] and P. V. AJAYA KUMAR[***]

Agronomy and Soil Science Division, Central Institute of Medicinal and Aromatic Plants, Lucknow 226015, India
[*]*Materials Science Division, North East Institute of Science and Technology, Jorhat, Assam, India*
[**]*Molecular Bioprospection Division, Central Institute of Medicinal and Aromatic Plants, Lucknow 226015, India*
[***]*Analytical Division, Central Institute of Medicinal and Aromatic Plants, Lucknow 226015, India*
✉ *Corresponding author: Puja Khare, kharepuja@rediffmail.com*

Received May 31, 2016

Isolation of microcrystalline cellulose (MCC) from distilled waste of *Cymbopogon winterianus* was performed by two different methods: acid hydrolysis and ultrasound-assisted TEMPO (2,2,6,6-tetramethyl piperidine 1-oxyl) oxidation. The MCC obtained was characterized by Fourier-transform infrared spectroscopy (FT-IR), scanning electron microscopy (SEM), thermogravimetric analysis (TGA), X-ray powder diffraction (XRD), particle size and zeta potential analyses. The results revealed that the cellulose particles obtained by the above-mentioned methods has a rod shape and micro size. The MCC achieved by TEMPO oxidation had a smaller particle size and higher aspect ratios compared to that obtained by acid hydrolysis. The results demonstrated that the MCC prepared by acid hydrolysis and TEMPO oxidation had a crystallinity of 86 and 77%, respectively. The *in-vitro* cytotoxic study revealed that both MCC materials obtained from *Cymbopogon winterianus* were non-toxic. The study demonstrated a novel approach for using aromatic residues as a potential feedstock for obtaining microcrystalline cellulose. The results suggested that the thus-prepared MCC could be of interest for different industrial applications, specifically in the biomedical field.

Keywords: *Cymbopogon winterianus*, microcellulose, TEMPO oxidation, acid hydrolysis, cell viability

INTRODUCTION

Plant-derived cellulose has been considered a ubiquitous and naturally abundant organic compound, consisting of a linear chain of several hundreds to over ten thousand β glucose units. These cellulosic chains are biosynthesized and self-assessed into microfibrils, having crystalline and amorphous domains.[1] Cellulose crystals (CC) can be obtained by the removal of the amorphous regions through hydrolysis with acids or enzymes, or by mechanical separation. Crystalline cellulose offers a remarkable reinforcing capability, excellent mechanical properties and low density. Hence, it has attracted significant research interest in the last 20 years. It has been widely used to enhance the properties of various host matrices in the preparation of nano-composites.

Various methods have been used for the isolation of microcrystalline cellulose from plant as well as bacterial sources. These comprise acid hydrolysis,[2,3] ultrasonic techniques,[4] enzyme assisted hydrolysis,[5] 2,2,6,6-tetramethylpiperidine-1-oxyl (TEMPO) mediated oxidation[6,7] and combinations of these techniques.[8-10] TEMPO mediated oxidation of cellulose has recently gained increased attention. When TEMPO/NaBr/NaClO oxidation is applied to native celluloses, the C_6 primary hydroxyls of cellulose can be entirely or selectively converted to sodium carboxylate groups.[11] Ultrasonication assisted TEMPO oxidation could further facilitate the disintegration of cellulosic fibers into single crystalline cellulosic fibers.

Cymbopogon winterianus Jowitt (Poaceae), known as Java citronella, is mainly used as an insect repellent and air freshener.[12] The oil extract from citronella has been used as a fragrance

component in cosmetics and as a flavor ingredient in the food industry. The high growth rate and cultivation of citronella (CT) on marginal land provides a high economic gain with low input, which promotes its enhanced cultivation. The increase in cultivation generates an enormous quantity of distilled waste every year after oil extraction, which is known to be rich in cellulosic content.[13] Reasonable and sustainable utilization of the distilled waste of citronella would be of great interest and would reduce the adverse environmental impact of such activities as biomass burning. The isolation of natural fibrils, specifically nanocellulose, from this waste would be helpful in creating a new value-added product, which can be used for various applications.

The major objective of the present study was to explore the feasibility of using distilled waste of citronella (DWC) as a new possible lignocellulosic predecessor for producing nanocellulose, which could be used as a value-added product in food, pharma and cosmetics industries. Acid hydrolysis and ultrasound-assisted TEMPO oxidation were used for isolation of MCC from DWC. The isolated MCC was analyzed in order to explore the effects of different extraction processes on its properties. In the study, the notations CT-CC, CT-AH and CT-TO were used for citronella cellulose, acid hydrolyzed cellulose and TEMPO oxidized cellulose, respectively. The properties of the cellulosic fibers, such as thermal stability, crystallinity, hydrogen bonding and surface functionality, were evaluated using thermogravimetric analysis (TGA), X-ray diffraction and FT-IR analyses. An *in-vitro* study was conducted to investigate the effects of CT-TO and CT-AH on cell viability in order to assess their suitability for biomedical applications.

EXPERIMENTAL

Materials

The chemicals used in the study were the following: toluene (Merck), ethanol (Merck), sodium hydroxide, hydrogen peroxide (Merck), sodium borate (Merck), nitric acid (Merck) acetic acid (Merck) and TEMPO (Sigma Aldrich). All of them were of analytical grade and a purity of 98-99%.

Extraction of cellulose from plant fibers

The distilled waste of citronella (*Cymbopogon winterius*) (DWC) was received from an oil extraction unit of CSIR-CIMAP (Central Institute of Medicinal and Aromatic Plants), Lucknow, India, was oven-dried at 80 °C for 24 hours and chopped. The extractive free biomass (DWC) was characterized to find its cellulose content.[14] The yield was calculated.

For the dewaxing and delignification process, 10 g of distilled waste of citronella was taken and Soxhlet extraction was performed for 24 hours using toluene/ethanol (2:1 v/v). The dewaxed fibers were filtered, washed with ethanol for 30-60 minutes and dried.

For the extraction of cellulose fibers, the extractive free plant biomass was subjected to a pretreatment with 0.1 M NaOH in a 50% volume of ethanol at 45 °C for 3 hours under continuous agitation. Then, bleaching was performed at pH = 11.5 (buffer solution) and 45 °C with different concentrations of hydrogen peroxide: (a) 0.5% H_2O_2, (b) 1.0% H_2O_2, (c) 2.0% H_2O_2 and (d) 3.0% H_2O_2, for 3 hours under continuous agitation. After that, the final treatment was carried out with 10% w/v NaOH – 1% w/v $Na_2B_4O_7.10\ H_2O$ at 28 °C for 15 hours, under continuous agitation, according to the methods described by Sun and Sun.[15] A certain amount of the isolated cellulosic fibers was stored for analysis. The rest of the sample was freeze-dried (Labconco freeze dryer-free zone 2.5 plus-7522800-USA).

Acid hydrolysis of cellulose

For preparing microcellulose, cellulose hydrolysis was carried out with 64% (w/w) sulfuric acid at 45 °C for 45 minutes under constant stirring. Immediately after the acid hydrolysis, the suspension was diluted 10-fold with deionized water to quench the reaction. The extra water was decanted and the samples were subjected to mild ultrasonication. The suspension was centrifuged at 15000 rpm for 10 minutes to concentrate the cellulose and remove excess aqueous acid. The resultant precipitate was rinsed, re-centrifuged, and washed again with water until a constant neutral pH was achieved.[16]

TEMPO mediated oxidation of cellulose fibers

Oxidation of the extracted cellulose fibers was carried out using TEMPO (2,2,6,6-tetramethylpiperidine-1-oxyl radical) coupled with ultrasonication. Firstly, the fibers (10 g) were soaked in water overnight and then homogenized to obtain a uniform suspension of fiber of 1% consistency. TEMPO (0.11 $mmolg^{-1}$) and NaBr (0.617 g^{-1}) were dissolved in 50 mL deionized water. The pH of the fiber slurry was adjusted between 10-12 using 0.5M NaOH. The oxidation was started by adding NaOCl (3.75 mmol) and the TEMPO/NaBr solution to the fiber suspension. The reaction was stopped after 90 min by adding ethanol, the fibers were recovered through vacuum filtration and washed with distilled water until a neutral pH was achieved (the optimized time on the basis of yield). The fiber slurry was dialyzed for 5 days and then filtered and freeze-dried to quantify the yield of oxidized fiber.

Characterization of microcellulose

FT-IR was performed on a Thermo Scientific (NICOLET-380) infrared spectrophotometer, using the KBr method in the range of 4000 to 650 cm^{-1} with the resolution of 4 cm^{-1}.

The energy of the hydrogen bonds E for several OH stretching bands was calculated using Equation 1 reported by Ornaghi *et al.*:[17]

$$E = \frac{1}{k}\frac{v0 - v}{v} \quad (1)$$

where *v0* is the standard frequency corresponding to free OH groups (3650 cm^{-1}); *v* is the frequency of the bonded OH groups; and *k* is a constant ($1/k = 2.625 \times 10^2$ kJ). The hydrogen bond distances *R* are obtained using Equation 2, proposed by Ornaghi *et al.*:[17]

$$\Delta v = 4430 \times (2.84 - R) \quad (2)$$

where $\Delta v = v0 - v$; *v0* is the monomeric OH stretching frequency, which is taken to be 3600 cm^{-1}; and *v* is the stretching frequency observed in the infrared spectrum of the sample.

The structural (physical) analysis of the samples was evaluated by X-ray diffraction using a Rigaku X-ray diffractometer (ULTIMA IV, Rigaku, Japan) with a Cu Kα X-ray source (λ = 1.54056 Å) at a generator voltage of 40 kV and a generator current of 40 mA. The crystallinity indices (CI_{XRD} %) were calculated using Segal's equation:

$$CI_{XRD}\,(\%) = \frac{I_{200} - I_{am} \times 100}{I_{200}} \quad (3)$$

where I_{200} is the peak intensity at the (200) (2θ = 22.5°) plane and I_{am} is the minimum intensity at the valley between (200) and (101) planes (2θ = 18°).

The d-spacing between the crystal planes at the main peak was calculated using Bragg's law equation:

$$\lambda = 2d\sin\theta \quad (4)$$

where *d* is the distance between the crystal planes, θ is the Bragg angle and λ the X-ray wavelength.

The Scherrer equation (5) was used to calculate the crystal size (nm) of cellulose I structure with respect to the (200) plane:[18]

$$CS = \frac{0.9\lambda}{H\cos\theta} \quad (5)$$

where *CS* is the crystalline size, λ is the X-ray wavelength, *H* is the full-width at half-maximum (FWHM) and θ is the Bragg angle at the corresponding lattice plane.

The thermal behavior of the crystalline cellulose obtained from distilled waste of citronella was investigated using a Leco TGA 701 in aluminium pans. The samples were heated from 30 to 800 °C at a heating rate of 10 °C/min under nitrogen atmosphere. The weight changes were recorded against the heating temperature. The content of carbon, hydrogen, nitrogen and sulphur in the crystalline cellulosic was determined using a CHN Elemental Analyzer (Euro-Vector-EURO EA-3000).

The particle size distribution and zeta potential of the crystalline cellulose obtained were determined using a laser diffractometer (Malveran Mastersizer). The swelling index was determined by calculating the volume occupied by the sample before and after swelling. For this, 1 g of dried sample was placed in a cylindrical tube and then the volume occupied by the sample was noted down. After that, 25 mL of distilled water was added to the vessel and shaken vigorously and allowed to stand for 1 hour and then the increase in the volume was noted. The swelling index was calculated according to the method given by Amin *et al.*[19] and expressed in mlg^{-1} of the dried weight of sample.

For the analysis of COOH groups, the TEMPO oxidized sample (0.5 g) was immersed in 0.01M HCl to convert the cation into hydrogen ion. To the oxidized suspension, 50 mL of distilled water and 30 mL of 0.25 M calcium acetate were added. The mixture was allowed to stand for two hours and was shaken frequently to facilitate the interchange of ions. Then, 30 mL of the portion was withdrawn and titrated with 0.01M NaOH using a phenolphthalein indicator. The carboxyl content was calculated using the formula:

$$COOH\left(\frac{mmol}{g}\right) = \frac{\left(\frac{80}{30}\right) 0.01\text{M}.\,\text{V(NaOH)}}{\text{m}\left(1 - \frac{\text{w}}{100}\right)} \quad (6)$$

where *0.01 M* is the concentration of NaOH, *V(NaOH)* is the volume (mL) of the NaOH solution used for titration, *m* is the weight of treated fibers (g), and *w* is the moisture content.

Cell viability using the MTT assay

The cytotoxicity of CT-TO and CT-AH was assessed in peritoneal macrophage cells using the 3-(4,5-dimethylthiazol-2-yl)-2,5-diphenyltetrazolium (MTT) assay.[20,21] Peritoneal macrophage cells (0.5 x 10^6 cells/well) isolated from mice were suspended in RPMI 1640 medium (Sigma, USA), containing 10% heat-inactivated fetal bovine serum (Gibco, USA) and incubated in a culture 96-well plate at 37 ºC in 5% CO_2 in an incubator and left overnight to get attached. The cells were treated (1, 10, 100 µgmL^{-1}) and incubated for 24 h at 37 ºC in 5% CO_2. After incubation, 20 µL of MTT solution (5 mg/ml in PBS) was added to each well and left for 4 hours, followed by medium removal and cell solubilization in DMSO (100 µL) for 10 minutes. The culture plate was placed on a micro-plate reader (Spectramax; Molecular Devices, USA) and the absorbance was measured at 550 nm. The amount of color produced is directly proportional to the number of viable cells. Cell cytotoxicity was calculated as the percentage of MTT absorption as follows: Percentage (%) of survival = (mean experimental absorbance/mean control absorbance×100).

RESULTS AND DISCUSSION

The DWC consists of 30% cellulose, 30% hemicellulose and 18% lignin (Table 1). Meanwhile, the citronella plant is reported to have

values of 35% cellulose, 33% hemicellulose and 27% lignin,[22] which supports the considerable amount of cellulose in DWC. The yields of crystalline celluloses obtained by TEMPO oxidation and acid hydrolysis were of 80±1.1 and 83±1.6%. Therefore, it can be concluded that DWC is a good source for cellulose extraction.

Fourier Transform Infrared (FT-IR) spectroscopy

Hydrogen bonding and functional groups in cellulose (CC), CT-AH and CT-TO were assessed by Fourier Transform Infrared spectroscopy analysis (Fig. 1). The information regarding the hydrogen bonds between the cellulose chains was obtained using Equations 1 and 2. Strong bands at 3340 cm^{-1} and 2900 cm^{-1} in the DWC crystalline cellulose were due to the stretching vibration of O-H groups and symmetric C-H vibrations, respectively.[23] The peak at 1029 cm^{-1} was due to C-O-C pyranose ring skeleton vibrations. The peaks around 1120 and 665 cm^{-1} were attributed to the stretching vibrations of intermolecular ester bonding and the C-OH out-of-plane bending mode. The increase in intensity of the stretching band at 1619 cm^{-1} in the spectrum of CT-TO was attributed to the formation of carboxylic groups during oxidation. On the other hand, the CT-TO absorption patterns maintain the peak at 1734 cm^{-1} due to the presence of carboxylic acid groups.[24,67]

FT-IR spectroscopy was also used to assess the ratios of two natural allomorphs of cellulose, *i.e.* the one-chain triclinic (Iα) and two-chain monoclinic (Iβ) unit cells. These allomorphs may influence the crystal pattern of cellulose, also leading to significant alteration of other properties. The fractions of Iα in CT-TO and CT-AH were almost similar (Table 1).

The hydrogen bond intensity (HBI) in CC was calculated by the ratio between the absorption bands at 3400 cm^{-1} and 1320 cm^{-1} (Table 2). The fraction of the hydrogen bonded C=O (HBY) was compared by dividing the peak area of 1720 cm^{-1} (hydrogen bonded C=O groups) by 1746 cm^{-1} (free C=O groups). Vibrations due to intra-molecular hydrogen bonding in the OH band appear at around 3432 cm^{-1} in cellulose. It is evident from Table 3 that HBI was higher for the CT-TO samples. It could be due to the presence of higher charges on the surface of CT-TO. The fraction of hydrogen bonding in C=O (HBY) is also shown in Table 3.

As TEMPO oxidized cellulose had more hydrogen bonded C=O, the values of HBY showed a concordant pattern with surface charge. It is generally accepted that hydrogen bonding is a crucial factor for the development of conformational and mechanical properties. The bond length of O (6) H---O (3) is estimated to have a length of 2.79 A°.[25] CT-TO had slightly higher bond length, indicating that the intrinsic bond lengths of MCC obtained from DWC could be modified by different routes of isolation.

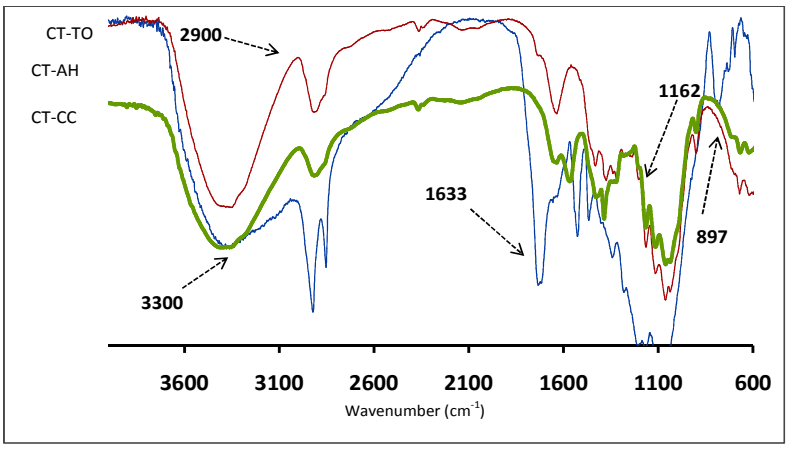

Figure 1: FT-IR spectra of cellulose (CC), acid hydrolyzed (CT-AH) and TEMPO oxidized (CT-TO) MCC

Table 1
Chemical constituents of biomass and yield of cellulose and MCC by TEMPO oxidation (TO) and acid hydrolysis (AH)

	Constituents			Yield (%)		
	Cellulose	Hemicellulose	Lignin	Cellulose	TO	AH
CT	30±1.2	30±1.4	18±1.1	85±2.1	80±1.1	83±1.6

Table 2
Properties of MCC obtained by acid hydrolysis and TEMPO oxidation

Sample	Length (nm)	Width (nm)	Z (mv)	SI	CI_{XRD} (%)	I_α	Cs	COOH (mmol/g)	SO_3^- (mmol/g)
CC	-	-	-	-	54±1	-	-	-	-
CT-AH	102±5.1	65±2.8	-25.0±1	0.83±0.08	86±1	0.52±.003	0.20±.004	0.53±0.03	1.13±0.02
CT-TO	84±2.4	14±1.1	-37.0±3	5.00±0.89	77±2	0.51±.007	0.23±.007	9.34±1.2	ND

SI: Swelling index, Cs: Crystallite size

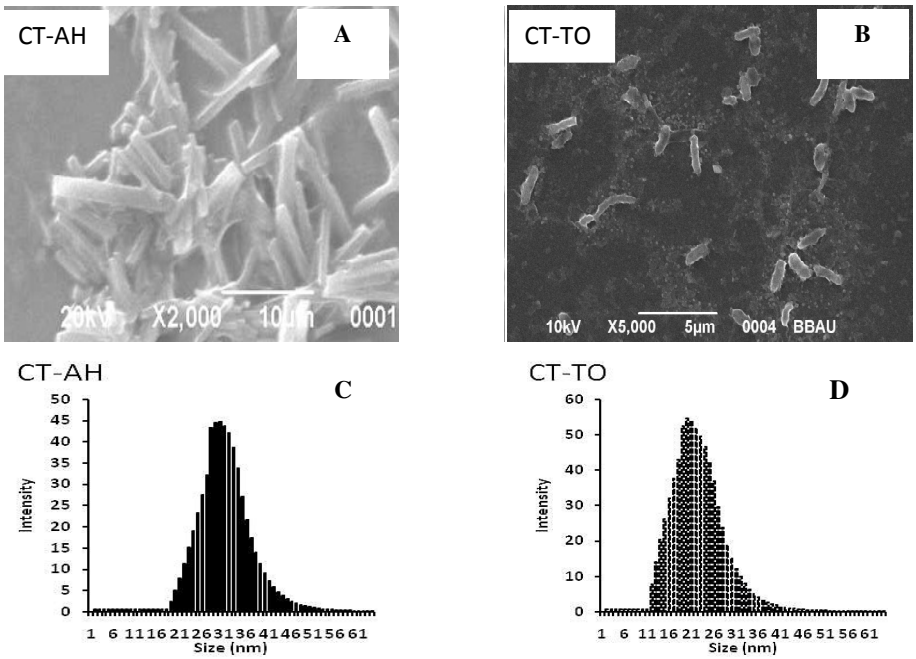

Figure 2: SEM images (A and B) and particle size distribution (C and D) of CT-AH and CT-TO

Table 3
Hydrogen bonding derived from FT-IR spectra

Sample	EH (KJ)	R (A°)	HBI	HBY
CT-AH	17.42708	2.78605	0.940552	0.134203
CT-TO	18.52083	2.782664	1.012977	0.151606

HBI: hydrogen bond intensity, HBY: hydrogen bond yield

Particle size and surface charge

The particle size analysis presented in Figure 2 and Table 2 revealed that CT-TO had lower particle size and higher aspect ratios. This may be explained by the shortening of fiber length caused by ultrasonication during TEMPO mediated oxidation, which depolymerizes the glycosidic linkages of cellulose. The constant bundle size might be explained by the accumulation of charges, which favored a uniform size. Typically,

a zeta potential of around 50 mV is needed for good colloidal stability. Our samples have a zeta potential in the range of 25-45 mV, therefore, the formation of microfibril aggregates was observed. According to the classical colloidal theory, the aggregation of primary particles cannot occur until the charge of the aggregate is high enough. The collision of two highly charged aggregates does not lead to a larger aggregate. A similar process applies here, where at a bundle size of about 1-10 μm, the total charge of the bundles was large enough to counteract the short-range attraction of van der Waals forces. It could be responsible for the inhibition of bundle growth.

The results of SEM revealed that CT-AH exhibited aggregated crystals, while CT-TO showed fibrillated surface. However, the SEM analysis results did not corroborate with the particle size analysis in the present study. The difference between the SEM image data and particle size distribution was due to the processing of the cellulosic crystals. The particle size was measured in liquid phase, while the SEM images were taken after freeze-drying. It is possible that the hydrogen bonding between cellulosic fibers could lead to aggregation. Peng *et al*. also reported that after freeze-drying the width and length of fiber may remain from micrometer to millimeter in size.[26]

The influence of surface charge on cellulose aggregation and size can be assessed by zeta potential and functional group analysis of cellulose fibers (Table 1). It revealed that the CT-TO had higher zeta potential, compared to CT-AH, due to its more attractive nature, which could lead to less aggregation and more uniform dispersion of microcellulose. High carboxylic content on the surface may cause more electrostatic repulsion between fibrils and helps maintain a homogenous dispersion for a long time.

Swelling properties

The swelling ratio of the cellulose is a very important feature for the development of any cellulosic fibers or hydrogels for various industrial applications, such as drug delivery, antibacterial films and hydrogels, as it plays an important role in the release of active compounds in various media.[27,28] It is evident from the swelling index values shown in Table 1 that the ultrasonication-assisted TEMPO oxidation route could produce CC with a higher swelling index. The samples exhibited 3-5 fold higher swelling compared to the original dry material. On the contrary, soaking CT-AH in the water solution led to a volume increase of only 0.5 to 0.8 times compared to the dry CT-CC. It may be due to the introduction of more hydrophilic carboxyl groups on the surface. As soon as cellulosic fibers are immersed into water, the water is transferred into absorbing areas, such as cracks, cavities on the surface, which results in the swelling of cellulose.[29] The swelling properties of the samples under study suggest that CT-TO could be applied to form cellulose beads with alkali metals, such as Ca^{2+}, which have been proposed for a range of biotechnological applications. This would widen the applicability of microcellulose as a biomaterial.[30]

XRD analysis

In order to investigate the effect of the isolation route and plant source on the crystalline structure of cellulose, the X-ray diffraction patterns of the samples were examined (Fig. 3). Cellulose fibers obtained from DWC presented diffraction peaks at 2θ = 14.5°, 16.2°, 22.6° and 34°, belonging to miller indices of -110, 110, 200 and 004, respectively, in the crystal structure of cellulose I. The peaks at 12.1 and 19.8° were assigned to the crystalline plane of -110 and 110 of cellulose II. It reflects that both treatments preserved the main crystal structure of cellulose, in accordance with the FT-IR data. The crystalline index calculated for all CCs using Equation 3 (Table 2) ranged from 77 to 84%. The crystallinity indexes of CT-AH (86%) and CT-TO (77%) were higher than the value of 54% for the extracted cellulose. This was attributed to the progressive removal of the cellulose in the amorphous regions. In addition, the value of CT-TO was lower than that of CT-AH, because of partial damage of the crystalline structure of cellulose during the treatment with TEMPO assisted by ultrasonication. Therefore, two types of high crystalline microcellulose were obtained by two different processes from distilled waste of citronella. It has been reported that high crystalline microcellulose could be more effective in improving the mechanical properties of composite materials, since higher crystallinity is associated with higher tensile strength of the material.[31] Hence, CT-AH is more suitable for the enhancement of the mechanical properties of any composite. The crystal size of CT-TO was higher compared to that of CT-AH. Higher crystallinity means an effective elimination of the amorphous cellulose from the fibers, leaving crystalline

cellulose. As a consequence, the range of crystallite size was decreased. In the case of TEMPO oxidized cellulose, the surface modification contributed to the formation of a new amorphous region around the crystalline cellulose by hydrogen bonds with the hydroxyl groups present in the exterior chains of the molecular wall. Hence, a slight increase in the crystallite size occurring as a result of the addition of carboxylate to the crystalline region is reasonable.[32]

Thermal stability

TGA and differential thermogravimetric (DTG) curves of CT-CC, CT-TO and CT-AH are shown in Figure 4A and B, respectively. The initial small weight loss (9 to 12%) at a low temperature (100-150 °C) corresponded to the evaporation of absorbed water. The thermal decomposition peaks of the maximum weight loss appeared at 200, 330 and 300 °C for CT-CC, CT-TO and CT-AH, respectively. However, maximum rates of weight loss were of 2.9, 5.5 and 1.9 for CT-CC, CT-TO and CT-AH, respectively. All of the above results indicated that the thermal stability of CT-TO was lower than that of CT-AH, the samples showing different thermal degradation patterns. For CT-TO, there was a slight weight loss up to 270 °C, and a drastic loss at 270-440 °C, followed by slow weight losses up to 800 °C. For CT-AH, there was drastic loss at 200-300 °C and slow weight losses up to 480 °C, followed by a sudden loss from 480 to 520 °C. These results are similar to those reported in our previous publications.

The onset decomposition temperature of the extracted cellulose and CT-AH, at 200 and 180 °C, respectively, was lower than that of CT-TO at 280 °C. This lower degradation temperature for CT-CC and CT-AH could be due to the hemicellulose component. Hemicelluloses embedded within and between the cellulose fibrils decomposed before lignin and cellulose because of the presence of acetyl groups in the hemicellulose molecules.[33]

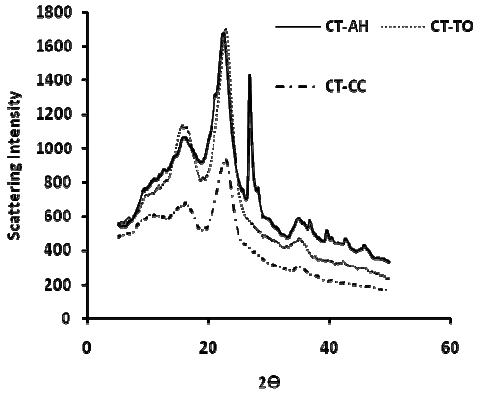

Figure 3: XRD spectra of microcellulose

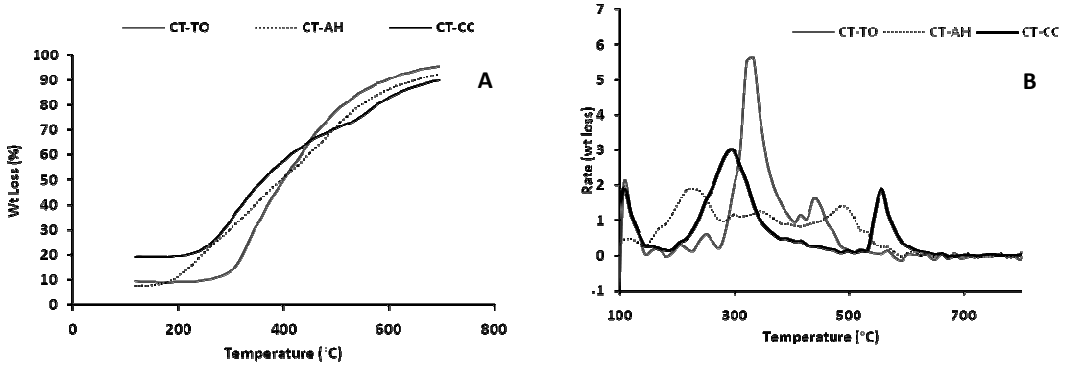

Figure 4: TGA (A) and DTG (B) curves of microcellulose

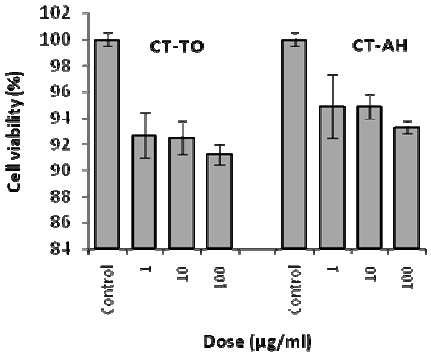

Figure 5: *In-vitro* cytotoxicity effects of CT-TO and CT-AH on cell viability

CT-TO exhibited higher thermal stability at the decomposition temperature of 180 °C. It could be due to higher hydrogen bonding on the CT-TO surfaces, which resist the devolatilization of surface functional groups. At the onset of degradation, the thermal stability was different for the three types of celluloses, which obviously showed differences in their degradation behaviors.

As for the MCC obtained by sulfuric acid hydrolysis, the degradation occurred within a wider temperature range and showed two well-separated pyrolysis processes. The first process in CT-AH involved a weight loss of about 47% (from 180 to 285 °C), while the weight loss in the second process decreased to 43% (from 285 °C to 485 °C). The decomposition of MCC occurring at lower temperatures, from 180 to 285 °C, might also indicate faster heat transfer in MCC. The better thermal conductivity of CT-CC might be ascribed to smaller phonon scattering in the bundle of crystallized cellulose chains than in the amorphous random chains in cellulose. The second process occurring from 285 °C to 485 °C could be related to the slow charring process of the solid residue. It describes the consecutive degradation reaction occurring in the cellulose crystalline interior at higher temperatures.

In the case of the microcrystalline cellulose obtained by ultrasonication-assisted TEMPO oxidation, the degradation occurred within a wider temperature range and showed three well-separated pyrolysis processes. The first process involved a weight loss of about 16% (from 180 to 285 °C), while the weight loss in the second process increased to 56% (from 285 °C to 392 °C) and then decreased to 14% (from 392 °C to 485 °C). Here, the higher weight loss in second process was due to the devolatilization of carboxylic groups present on the surface of cellulose.

***In-vitro* study of cell viability**

The *in-vitro* effect of CT-TO and CT-AH on cell viability in peritoneal macrophage cells isolated from mice was evaluated using the MTT assay. None of the two microcellulosic materials caused significant mortality, showing up to 94% cell survivability. No significant changes in % live cells were observed ($p < 0.05$) at any concentration of the treatment, when compared with normal cells (Fig. 5). No significant toxic effects were noted for the prepared materials, which confirmed the idea that cellulosic materials can be considered as the best biocompatible biodegradable material to be used in the biomedical field. The MTT assay demonstrated no significant difference in cell viability between CT-AH and CT-TO, despite their structural differences.

CONCLUSION

The present study investigated the MCC obtained from distilled waste of *Cymbopogon winterianus*. CT-TO exhibited excellent swelling properties, while CT-AH presented good crystallinity and thermal stability. The *in-vitro* study of the effects of CT-TO and CT-AH application on cell viability in peritoneal macrophage cells isolated from mice suggested that the materials presented no significant toxicity. The results thus demonstrated that distilled waste of citronella (DWC) could be an excellent option for the production of crystalline cellulose at an industrial scale, and the MCC obtained from it could be a good candidate for biomedical and mechanical applications.

ACKNOWLEDGEMENTS: The work was supported by the Council of Scientific and Industrial Research, New Delhi. The authors are thankful to Mr. T. Das, NEIST, Jorhat, for the TGA analysis and to Dr. A. K. Diwedi, CDRI Lucknow, for the particle size analysis of the samples.

REFERENCES

[1] C. J. Chirayil, J. Joy, L. Mathew, M. Mozetic, J. Koetz *et al*., *Ind. Crop. Prod*., **59**, 27 (2014).
[2] M. A. S. Azizi Samir, F. Alloin and A. Dufresne, *Biomacromolecules*, **6**, 612 (2005).
[3] N. Johar, I. Ahmad and A. Dufresne, *Ind. Crop. Prod*., **37**, 93 (2012).
[4] H. Wang, D. Li and R. Zhang, *BioResources*, **8**, 1374 (2013).
[5] P. Satyamurthy and N. Vigneshwaran, *Enzyme Microb. Technol*., **52**, 20 (2013).
[6] T. Saito and A. Isogai, *Biomacromolecules*, **5**, 1983 (2004).
[7] Y. Okita, T. Saito and A. Isogai, *Holzforschung*, **63**, 529 (2009).
[8] G. Siqueira, S. Tapin-Lingua, J. Bras, D. da Silva Perez and A. Dufresne, *Cellulose*, **17**, 1147 (2010).
[9] P. Chen, H. Yu, Y. Liu, W. Chen, X. Wang *et al*., *Cellulose*, **20**, 149 (2013).
[10] H. Lu, Y. Gui, L. Zheng and X. Liu, *Food Res. Int*., **50**, 121 (2013).
[11] N. Lin, C. Bruzzese and A. Dufresne, *Appl. Mater. Interfaces*, **4**, 4948 (2012).
[12] M. Silva, R. Ximenes, J. da Costa, L. K. M. Leal, A. de Lopes *et al*., *Arch. Pharmacol*., **381**, 415 (2010).
[13] M. Lwako, K. J. Baptist and K. B. Joseph, *Int. J. Chem. Eng. Appl*., **4**, 324 (2013).
[14] D. M. Updegraff, *Anal. Biochem*., **32**, 420 (1969).
[15] R. Sun and X. Sun, *Carbohyd. Polym*., **49**, 415 (2002).
[16] D. Mishra, V. Yadav, P. Khare, M. R. Das, A. Meena *et al*., *Curr. Top. Med. Chem*., **16**, 2026 (2016).
[17] H. L. Ornaghi, M. Poletto, A. J. Zattera and S. C. Amico, *Cellulose*, **21**, 177 (2014).
[18] P. Scherrer, *Nachr. Ges. Wiss. Gottingen*, **2**, 96 (1918).
[19] M. C. I. M. Amin, N. Ahmad, N. Halib and I. Ahmad, *Carbohyd. Polym*., **88**, 465 (2012).
[20] S. Sharma, S. K. Chattopadhyay, D. K. Yadav, F. Khan, S. Mohanty *et al*., *Eur. J. Pharm. Sci*., **47**, 952 (2012).
[21] M. V. Berridge and A. S. Tan, *Arch. Biochem. Biophys*., **303**, 474 (1993).
[22] K. J. Baptist, *Int. J. Sci. Technol. Res*., **2**, 146 (2013).
[23] F. Pelissari, P. A. Sobral and F. Menegalli, *Cellulose*, **21**, 417 (2014).
[24] T. Nikolic, J. Milanovic, A. Kramar, Z. Petronijevic, L. Milenkovic *et al*., *Cellulose*, **21**, 1369 (2014).
[25] D. Ciolacu, J. Kovac and V. Kokol, *Carbohyd. Res*., **345**, 621 (2010).
[26] Y. Peng, D. J. Gardner, Y. Han, A. Kiziltas, Z. Cai *et al*., *Cellulose*, **20**, 2379 (2013).
[27] G. Chinga-Carrasco and K. Syverud, *J. Biomat. Appl*., **29**, 423 (2014).
[28] Y. Qing, R. Sabo, J. Zhu, U. Agarwal, Z. Cai *et al*., *Carbohyd. Polym*., **97**, 226 (2013).
[29] J. Praskalo, M. Kostic, A. Potthast, G. Popov, B. Pejic *et al*., *Carbohyd. Polym*., **77**, 791 (2009).
[30] K. Syverud, G. Chinga-Carrasco, J. Toledo and P. G. Toledo, *Carbohyd. Polym*., **84**, 1033 (2011).
[31] B. Deepa, E. Abraham, B. M. Cherian, A. Bismarck, J. J. Blaker *et al*., *Bioresource Technol*., **102**, 1988 (2011).
[32] E. Robles, I. Urruzola, J. Labidi and L. Serrano, *Ind. Crop. Prod*., **71**, 44 (2015).
[33] R. M. Sheltami, I. Abdullah, I. Ahmad, A. Dufresne and H. Kargarzadeh, *Carbohyd. Polym*., **88**, 772 (2012).